An Enhanced Optimal PV and Battery Sizing Model for Zero Energy Buildings Considering Environmental Impacts

Mahdi Mehrtash, Florin Capitanescu, Per Kvols Heiselberg, Thomas Gibon, and Alexandre Bertrand

***Abstract*—The important focus of the energy strategy of the European Union relies on the concept of zero energy building (ZEB), which is, by definition, a building that roughly produces yearly as much renewable energy as it consumes. This article proposes an enhanced mixed-integer nonlinear programming model for optimal sizing of photovoltaic (PV) and battery energy storage systems to comply with the definition of a ZEB. A salient novel feature of the proposed model is that it factors in the environmental impacts, computed through rigorous life cycle assessment methodology, of buying electricity from the grid and manufacturing battery and PV systems. Furthermore, an adjustable parameter is introduced to make the model adaptive from the perspective of the building owner's willingness-to-pay for environmental impacts. The proposed model is then rigorously reformulated, managing to accumulate its nonlinearity in only one constraint per time interval. Eventually, the reformulated model is linearized to a mixed-integer linear programming model using the McCormick relaxation technique. The case study conducted on archetypal buildings in Luxembourg reveals that the proposed McCormick-based linear model is able to provide high accuracy results with reasonable computational effort.**

***Index Terms*—Battery storage system, environmental impacts, McCormick envelops, mixed-integer nonlinear programming, optimal photovoltaic (PV) and battery sizing, zero energy building (ZEB).**

Manuscript received May 11, 2020; revised July 29, 2020; accepted September 2, 2020. Date of publication September 8, 2020; date of current version November 19, 2020. Paper 2020-SECSC-0821.R1, presented at the 2020 IEEE Texas Power and Energy Conference, College Station, TX, USA, Feb. 6–7, and approved for publication in the IEEE TRANSACTIONS ON INDUSTRY APPLICATIONS by the Renewable and Sustainable Energy Conversion Systems Committee of the IEEE Industry Applications Society. This work was supported by the Luxembourg National Research Fund (FNR) under contract C18/SR/12676686, in the frame of gENESiS project. *(Corresponding author: Mahdi Mehrtash.)*

Mahdi Mehrtash is with the Luxembourg Institute of Science and Technology (LIST), ERIN, Belvaux L-4422, Luxembourg, and also with the Faculty of Applied Science, University of British Columbia, Vancouver, BC V6T 1Z2, Canada (e-mail: mahdi.mehrtash@list.lu).

Florin Capitanescu, Thomas Gibon, and Alexandre Bertrand are with the Luxembourg Institute of Science and Technology (LIST), ERIN, Belvaux L-4422, Luxembourg (e-mail: florin.capitanescu@list.lu; thomas.gibon@list.lu; alex.bertrand@list.lu).

Per Kvols Heiselberg is with the Department of Civil Engineering, Aalborg University, DK-9220 Aalborg Øst, Denmark (e-mail: ph@civil.aau.dk).

Color versions of one or more of the figures in this article are available online at https://ieeexplore.ieee.org.

Digital Object Identifier 10.1109/TIA.2020.3022742

NOMENCLATURE

Indices and Sets

t	Index of time interval (e.g., 8760 h per year).
e	Index for environmental impact categories.

Parameters

I_B^{initial}	Initial investment cost of the battery [€/kW·h].
I_B^{OM}	Operation and maintenance cost of the battery [€/kW·h].
$I_{\text{PV}}^{\text{initial}}$	Initial investment cost of the PV [€/kW·p].
$I_{\text{PV}}^{\text{OM}}$	Operation and maintenance cost of the PV [€/kW·p].
$\text{CRF}(i,n)$	Capital recovery factor.
$\text{CEI}(e)$	Cost of environmental impact e at interval t.
$\text{EIM}^{\max}$	Maximum limit for environmental impacts.
$\text{EP}(t)$	Electricity price [€/kW·h].
$\text{FIT}(t)$	Feed-in-tariff [€/kW·h].
i	Interest rate of financial investment.
n	Number of years of financial investment.
$P_{\text{PV}}(t)$	Active power generated by PV system at time interval t [kW].
$P_L(t)$	Active demand at time interval t [kW].
$\text{SOC}_{\min}/\text{SOC}_{\max}$	Minimum/maximum state of charge of the battery [p.u.].
Δt	Time interval duration (e.g., 1 h).
η_c, η_d	Charging/discharging efficiency of the battery and converter system.
$\alpha(t)$	Per unit PV output at time interval t.

Variables

C_B	Battery capacity [kW·h].
C_{PV}	PV capacity [kW·p].
$I_{\max}(t)/I_{\min}(t)$	Binary variables indicating that state of charge of the battery is reaching to its maximum/minimum at time interval t.
$I^+(t)$ / $I^-(t)$	Binary variables indicating that PV production is higher/lower than the active demand at time interval t.
$P^+(t)$/ $P^-(t)$	Excess/Deficit of active power at time interval t [kW].

$P_b(t)$/ $P_s(t)$	Active power buy from/sell to grid at time interval t [kW].
$P_c(t)$/ $P_d(t)$	Charging/discharging power of the battery at time interval t [kW].
$\mathrm{SOC}(t)$	State of charge of the battery at time interval t [p.u.].
$\omega(t)$	Auxiliary variable for McCormick relaxation.

I. Introduction

THE emission of greenhouse gases (particularly CO_2) is an unavoidable consequence of using fossil fuels to produce electricity. Buildings, as one of the key contributors to CO_2 emissions, are in charge of 40% of the final energy consumption and 36% of CO_2 emission in the European Union (EU). As a consequence, the idea of zero energy buildings (ZEBs) was promoted in the statement of the Energy Performance of Building's Directive in 2010 [1]. As stated in the directive, buildings are deemed part of the solution for both the emission of greenhouse gases and the security of supply.

Several definitions have been proposed for ZEBs. According to [1] and [2], we undertake that a ZEB is a building that produces as much electricity from renewable sources as it consumes yearly.

Building-integrated photovoltaic (PV) systems are the most common form of electricity production units in buildings, which are required to fulfill the definition of a ZEB. Albeit the yearly net electricity balance of a ZEB is close to zero, it still exchanges a significant bidirectional amount of electricity with the network due to the mismatch in time between the generation and consumption profiles. In this regard, the advantages of deploying a building-integrated battery energy storage (BES) system is widely studied in the literature [3]–[6].

The problem of finding the minimum investment cost of the PV and BES systems complying with the definition of a ZEB can be mathematically modeled as an optimization problem.

The problem of optimal BES sizing in residential ZEBs is analyzed in [3] relying on real-life data of a household in Portugal. It concludes that the designed BES system can diminish the energy export/import to/from the network by 76% and 78%, respectively, improving also the energy autarchy of the building. Studying a residential ZEB in Arizona, reference [7] presents a parametric approach to find the best capacity of the BES system in which the maximum net present value is achieved. It concludes that due to the unconformity between solar generations and peak demands, the studied ZEB is only able to reduce 37%–44% of the peak electricity purchases.

Reference [4] analyzes an optimal PV and BES sizing problem for commercial buildings, assuming that the electricity price is equal to the feed-in-tariff. However, this is not a sound hypothesis according to the price policy of most countries. The compensation of the mismatch between the generation and consumption patterns of ZEBs is addressed in [8]. Multiple modeling schemes for PV and BES systems, each of which focuses on a specific aspect of the model, are presented in works [5], [9]. Using dynamic simulation for electricity usage of ZEB houses in southern Kentucky, an optimal sizing of hybrid electric and thermal storage devices is presented in [10]. A BES sizing problem for residential ZEBs is proposed in [11]. The model prioritized storing the excess electric power in the battery rather than selling it to the grid. This is a suitable strategy because the electricity price is typically fixed, and it is higher than the feed-in-tariff for residential buildings. However, the mathematical model suffers from intractability to guarantee the prescribed optimality gap.

Using different optimization techniques, the number of works focused on the optimal sizing of ZEBs and smart homes has intensified recently. Considering only economical aspects, an optimal planning model for sizing PV and BES of smart homes is proposed in [12] based on particle swarm optimization (PSO) algorithm. Moreover, reference [13] proposed optimal sizing of energy storage devices to enhance the productivity of residential building-integrated PV systems. Ignoring environmental impacts, a PSO algorithm is applied to optimize the overall cost of the smart building. Similar to other heuristic algorithms, PSO can find a feasible solution in a short runtime but cannot guarantee the optimality or gauge the optimality gap of the obtained feasible solution. A dynamic programming-based optimal sizing of PV and BES capacity for residential homes is proposed in [14]. It is illustrated that the proposed dynamic programming approach outperforms heuristic methods considerably. However, the approach ignores the possibility of selling electricity to the grid and environmental impacts, and is not scalable.

The literature survey indicates that the most important research gap is to develop a rigorous yet scalable problem formulation for optimally sizing of PV and BES in ZEBs.

An aspect neglected in the literature is that both BES and PV systems generate environmental impacts, mostly during their manufacturing. Furthermore, the grid electricity is also a source of environmental impacts, which depend on the mix of technologies used to the power supply (e.g., nuclear, coal, gas, hydro, solar, wind, etc.) [15]. As climate change mitigation strategies are on top of the EU's environmental agenda, CO_2 and other greenhouse gas emissions are the most often inventoried lifecycle indicator. However, decarbonizing the power sector might require tradeoffs especially with land occupation or material requirements [16], [17]. How to factor in environmental impacts in the problem is another research gap.

To address the two knowledge gaps, this article significantly extends the previous authors' work [18], which only focused on profit-based optimal sizing of BES, in two respects: 1) joint optimal sizing of PV and BES systems and 2) consideration of environmental impacts. Accordingly, the key new contribution of this article is an enhanced (but scalable to large-scale planning problems) mathematical model for the optimal PV and BES sizing problem fulfilling the definition of ZEBs. A proposed enhancement, with respect to the existing models, is to enforce the priority to store the excess electric power in the battery instead of selling it to the grid. In addition, a new contribution is that the environmental impacts of buying electricity from the grid and manufacturing PV and BES systems are factored in through an adjustable parameter, which considers quantitatively the building owner's willingness-to-pay for environmental

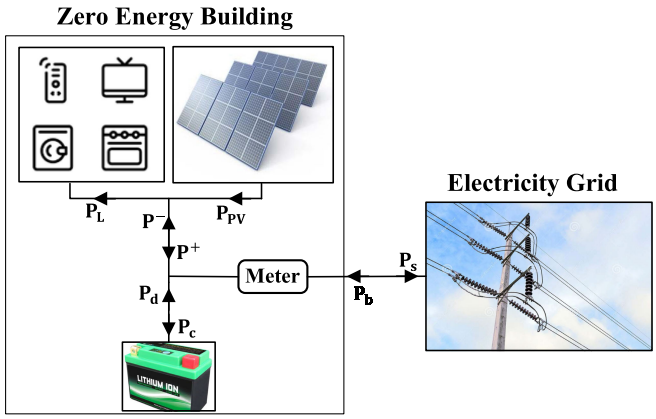

Fig. 1. Directions of power flows for zero energy building.

impacts. The efficacy of the model is demonstrated numerically using residential and commercial buildings from Luxembourg.

The remaining of this article is structured as follows. Section II describes the formulation of the proposed optimal PV and BES sizing problem. Section III presents a numerical case study. Section IV concludes this article.

II. Problem Formulation

For the sake of problem formulation clarity, Fig. 1 shows the power flow directions of the proposed optimal PV and BES sizing model. In terms of formulation, first, the optimal PV and BES sizing is modeled as a mixed-integer nonlinear programming (MINLP) problem. Next, the MINLP model is reformulated in a smart and rigorous way to accumulate all nonlinear terms in a single bilinear constraint per time interval. Finally, the bilinear constraint is linearized using the McCormick relaxation technique allowing us to obtain a scalable mixed-integer linear programming (MILP) model.

A. MINLP Model

The objective function of the optimal PV and BES sizing problem is expressed by (1). It contains four terms: investment/operation and maintenance cost of the battery storage, investment/operation and maintenance cost of the PV system, cost of buying electricity from the grid, and revenue of selling electricity to the grid.

$$\min_{(C_B,C_{\rm PV})} \Bigg\{ \mathrm{CRF}(i,n).(I_B^{\rm initial}+I_B^{\rm O\&M}).C_B + \mathrm{CRF}(i,n).(I_{\rm PV}^{\rm initial}+I_{\rm PV}^{\rm O\&M}).C_{\rm PV} + \Delta t.\left(\sum_{\forall t} P_b(t).\mathrm{EP}(t) - \sum_{\forall t} P_s(t).\mathrm{FIT}(t)\right)\Bigg\} \quad (1)$$

Decision variables of the optimization model are the size of the battery storage C_B (in kW·h) and the size of the PV system $C_{\rm PV}$ (in kW·p). Parameters $I_B^{\rm initial}$ in €/kW·h and $I_{\rm PV}^{\rm initial}$ in €/kW·p represent initial investment costs of the battery storage and the PV system, while $I_B^{\rm OM}$ and $I_{\rm PV}^{\rm OM}$ are the corresponding operation and maintenance costs. Variables $P_b(t)$ and $P_s(t)$, which are in kW, represent the amount of electricity bought from the grid and electricity sold to the grid at time interval t, respectively. The assumed duration of time intervals (e.g., 1 h) is expressed by Δt. Parameters $\mathrm{EP}(t)$ and $\mathrm{FIT}(t)$ in €/kW·h are the electricity price and the feed-in-tariff at time interval t, respectively. Note that the proposed objective function (1) is also valid in the case of time-varying electricity price and feed-in-tariff (i.e., $\mathrm{EP}(t)$ and $\mathrm{FIT}(t)$ can be different for diverse intervals).

Due to irreversible electrochemical changes, long-term usage of the battery results in performance degradation, e.g., increment of internal resistance, capacity reduction, and efficiency deterioration. Here, we consider the performance degradations of PV and BES systems as operation and maintenance costs, which are linearly dependent on the optimal sizes. Depending on the application, more sophisticated modeling of performance degradations might be desired, such as the physics-based model proposed by [19] for model predictive control of Lithium-Ion batteries.

The initial investment costs of the PV and BES systems (including the associated converter if required [20]) are assumed to be financed with an interest rate of i for a period of n years (similar to the warranty period of the PV and BES systems). Therefore, the capital recovery factor CRF can be obtained from (2) [21].

$$\mathrm{CRF}\ (i,n) = \frac{i(1+i)^n}{(1+i)^n-1}. \quad (2)$$

The excess and deficit of active power at time interval t are modeled as (3) and (4), respectively, which requires introducing binary variables. Parameters $\alpha(t)$ and $P_L(t)$ represent per unit PV output and electric power demand at time interval t, respectively. Binary variable $I^+(t)$ is equal to one if there is the excess of active power at time interval t, and it is equal to zero otherwise. Likewise, the binary variable $I^-(t)$ is equal to one if there is a deficit of active power at time interval t, and it is equal to zero otherwise. Constraints (5) and (6) model the positivity of the continuous variables $P^+(t)$ and $P^-(t)$, and constraint (7) expresses that both excess and deficit of active power cannot coexist at each time interval t

$$P^+\ (t) = (\alpha\,(t)\,.C_{PV} - P_L\,(t))\,.I^+\,(t)\,;\ \forall t \quad (3)$$

$$P^-\ (t) = (P_L\,(t) - \alpha\,(t)\,.C_{PV})\,.I^-\,(t)\,;\ \forall t \quad (4)$$

$$P^+\,(t) \geq 0;\ \forall t \quad (5)$$

$$P^-\,(t) \geq 0;\ \forall t \quad (6)$$

$$I^+\,(t) + I^-\ (t) = 1;\ \forall t. \quad (7)$$

The amount of active power that can be sold to the grid at time interval t is modeled as (8). Variable $P_c(t)$ is the charging power of the battery at time interval t; it can be obtained from (9). Similarly, the amount of active power that can be bought from the grid and the discharging power of the battery at time interval t are modeled as (10) and (11), respectively. Here, state of charge $(\mathrm{SOC})(t)$ in per unit represents the SOC of the battery at time interval t, and it is bounded by the minimum value $\mathrm{SOC}_{\min}$ and the maximum value $\mathrm{SOC}_{\max}$ as expressed in (12).

TABLE I
MEANING OF THE FOUR POSSIBLE STATUSES FOR EACH TIME INTERVAL

Status		I^+	I^-	I_{max}	I_{min}
1	Excess of active power exists and the available capacity of the battery is insufficient to fully store it.	1	0	1	0
2	Excess of active power exists and the available capacity of the battery is sufficient to fully store it.	1	0	0	0
3	Deficit of active power exists and the available energy of the battery is insufficient to fully supply it.	0	1	0	1
4	Deficit of active power exists and the available energy of the battery is sufficient to fully supply it.	0	1	0	0

Parameters η_c and η_d are the charging efficiency and discharging efficiency of the battery, respectively. Binary variable $\mathrm{I}_{\max}(t)$ is equal to zero if the battery has enough capacity to store the excess power completely without attaining its maximum SOC at time interval t, and it is equal to one otherwise. Similarly, the binary variable $I_{\min}(t)$ is equal to zero if the battery has enough energy to provide the deficit power completely without attaining its minimum SOC at time interval t, and it is equal to one otherwise.

$$P_s\ (t) = \left(P^+(t) - P_c(t)\right).I_{\max}(t);\ \forall t \tag{8}$$

$$P_c\ (t) = \left(\mathrm{SOC}_{\max} - \mathrm{SOC}(t-1)\right)\ \times \frac{C_B}{\eta_c.\Delta t};\ \forall t \tag{9}$$

$$P_b\ (t) = \left(P^-(t) - P_d(t)\right).I_{\min}(t);\ \forall t \tag{10}$$

$$P_d\ (t) = \left(\mathrm{SOC}(t-1) - \mathrm{SOC}_{\min}\right)\ \times \frac{\eta_d.C_B}{\Delta t};\ \forall t \tag{11}$$

$$\mathrm{SOC}_{\min} \le \mathrm{SOC}(t) \le \mathrm{SOC}_{\max};\ \forall t. \tag{12}$$

Four possible statuses exist for each time interval as detailed in Table I. Generally, having four binary variables results in $2^4 = 16$ possibilities. However, constraint (7) prunes eight infeasible possibilities. Constraints (13) and (14) prune the other four infeasible possibilities and set the feasibility region according to the desired status of Table I.

$$I_{\max}(t) \le 2 \times I^+(t);\ \forall t \tag{13}$$

$$I_{\min}(t) \le 2 \times I^-(t);\ \forall t. \tag{14}$$

Based on the set of feasible statuses shown in Table I, constraint (15) is proposed to model the SOC of the battery. According to (15), the value of $\mathrm{SOC}(t)$ is fixed to $\mathrm{SOC}_{\max}$ and $\mathrm{SOC}_{\min}$ for status 1 and status 3, respectively [see Table I and constraints (3)–(4)]. In addition, in status 2, the value of $\mathrm{SOC}(t)$ is equal to $\mathrm{SOC}(t-1)$ plus the excess power stored in the battery. Similarly, in status 4, the value of $\mathrm{SOC}(t)$ is equal to $\mathrm{SOC}(t-1)$ minus the deficit power provided by the battery. The energy preservation constraint (16) imposes that the SOC of the battery in the last interval is equal to the initial battery SOC.

$$\begin{aligned}\mathrm{SOC}\ (t) =\ & \mathrm{SOC}(t-1).(1 - I_{\max}(t) - I_{\min}(t)) \\ & + \frac{P^+(t).\Delta t.\eta_c}{C_B}(1 - I_{\max}(t)) - \frac{P^-(t).\Delta t}{\eta_d.C_B}(1 - I_{\min}(t)) \\ & + \mathrm{SOC}_{\max}.I_{\max} + \mathrm{SOC}_{\min}.I_{\min};\ \forall t\end{aligned} \tag{15}$$

$$\mathrm{SOC}\ (t = 0) = \mathrm{SOC}(t = \mathrm{last}). \tag{16}$$

The zero energy constraint and limitation of environmental impacts are modeled by linear constraints (17) and (18), respectively. According to (17), the annual electricity bought from the grid must be less or equal than the annual electricity sold to the grid. Constraint (18) limits the total environmental impacts of buying electricity from the grid and manufacturing BES and PV systems, where parameter $\mathrm{CEI}(e)$ represents the cost of environmental impact e in Pt/kW·h. As it will be illustrated by numerical case studies, $\mathrm{EIM}^{\max}$ is an adjustable parameter enabling to tradeoff the environmental impacts and the economical objective. It should be selected according to the building owner's willingness-to-pay for environmental impacts.

Note that the environmental constraint (18) aggregates the so-called "midpoint" lifecycle indicators, such as "climate change," "human toxicity," "particulate matter emissions," "eutrophication," or "land use." Recent initiatives to incorporate environmental indicators in system optimization problems include [22], which used a single-score indicator to convey the environmental pressure of the various power generation technologies

$$\sum_{\forall t} \Delta t.P_s(t) \ge \sum_{\forall t} \Delta t.P_b(t) \tag{17}$$

$$\begin{aligned}&\sum_{\forall t}\sum_{\forall e} \Delta t.P_b(t).\mathrm{CEI}_b(e) + \sum_{\forall e} C_B.\mathrm{CEI}_B(e) \\ &+ \sum_{\forall e} C_{\mathrm{PV}}.\mathrm{CEI}_{\mathrm{PV}}(e) \le \mathrm{EIM}^{\max}.\end{aligned} \tag{18}$$

To sum up, the proposed MINLP model for the optimal PV and BES sizing problem consists in minimizing the objective function (1) subject to (3)–(18). The decision variables of the model include the size of the battery C_B, size of the PV C_{PV}, the amount of electricity bought from the grid $P_b(t)$ and the amount of electricity sold to the grid $P_s(t)$.

Note that the nonlinear terms of the model are propagated in constraints (3), (4), (8)–(11), and (15). Therefore, reformulating the model in an equivalent way to reduce the number of nonlinear terms is desirable.

B. Reformulation of MINLP Model

Auxiliary variable $\omega(t)$ is defined in (19) to enable nonlinearity accumulation of the MINLP model. As it can be noticed from (19), the physical interpretation of the auxiliary variable $\omega(t)$ is the amount of energy that is stored in the battery at time interval t

$$\omega\ (t) = C_B\ .\mathrm{SOC}(t);\ \forall t. \tag{19}$$

A disjunctive technique is applied to linearize (3) as (20) and (21), where M is a sufficiently large constant (big-M technique).

When $I^+ = 0$, constraint (21) is nonbinding, and constraint (20) forces P^+ to be equal to zero. On the other hand, when $I^+ = 1$, constraint (20) enforces that $P^+(t) = \alpha(t).C_{\rm PV} - P_L(t)$ while (20) is nonbinding. Similarly, constraint (4) can be replaced by linear constraints (22) and (23)

$$0 \le P^+(t) \le M.I^+(t);\ \forall t \tag{20}$$

$$-M.\left(1 - I^+(t)\right) + \alpha(t).C_{\rm PV} - P_L(t) \le P^+(t) \le \alpha(t).C_{\rm PV} - P_L(t) + M.\left(1 - I^+(t)\right);\ \forall t \tag{21}$$

$$0 \le P^-(t) \le M.I^-(t);\ \forall t \tag{22}$$

$$-M.\left(1 - I^-(t)\right) + P_L(t) - \alpha(t).C_{PV} \le P^-(t) \le P_L(t) - \alpha(t).C_{PV} + M.\left(1 - I^-(t)\right);\ \forall t. \tag{23}$$

Applying the same technique and including the auxiliary variable $\omega(t)$, (8) and (9) are linearized as (24)–(26). Similarly, (10) and (11) are rewritten as linear constraints (27)–(29).

$$0 \le P_s(t) \le P_s^{\max}.I_{\max}(t);\ \forall t \tag{24}$$

$$-M(1 - I_{\max}(t)) + \left(P^+(t) - P_c(t)\right) \le P_s(t) \le \left(P^+(t) - P_c(t)\right) + M(1 - I_{\max}(t));\ \forall t \tag{25}$$

$$P_c(t) = [C_B.SOC_{\max} - \omega(t-1)] \times \frac{1}{\eta_c.\Delta t};\forall t \tag{26}$$

$$0 \le P_b(t) \le P_b^{\max}.I_{\min}(t);\ \forall t \tag{27}$$

$$-M(1 - I_{\min}(t)) + \left(P^-(t) - P_d(t)\right) \le P_b(t) \le + \left(P^-(t) - P_d(t)\right) + M(1 - I_{\min}(t));\ \forall t \tag{28}$$

$$P_d(t) = [\omega(t-1) - C_B.\mathrm{SOC}_{\min}] \times \frac{\eta_d}{\Delta t};\forall t \tag{29}$$

Last, constraint (15) is replaced by linear constraints (30)–(32) to model the four statuses enumerated in Table I. In status 1, when $I^+ = I_{\max} = 1$ and $I^- = I_{\min} = 0$, constraints (30) and (32) are inactive while (31) imposes that $\mathrm{SOC}(t) = \mathrm{SOC}_{\max}$. The same conclusion can be obtained from (15). Considering other status, it can be concluded that (30)–(32) are perfectly equivalent to (15).

$$-M(1 - I_{\max}(t)) + \mathrm{SOC}_{\max}.I_{\max}(t) \le \mathrm{SOC}(t) \le \mathrm{SOC}_{\max}.I_{\max}(t) + M(1 - I_{\max}(t));\ \forall t \tag{30}$$

$$-M(1 - I_{\min}(t)) + \mathrm{SOC}_{\min}.I_{\min}(t) \le \mathrm{SOC}(t) \le \mathrm{SOC}_{\min}.I_{\min}(t) + M(1 - I_{\min}(t));\ \forall t \tag{31}$$

$$-M.(I_{\max}(t) + I_{\min}(t)) + \omega(t-1) + \Delta t.(P^+(t).\eta_c - \frac{P^-(t)}{\eta_d}) \le \omega(t) \le \omega(t-1) + \Delta t.(P^+(t).\eta_c - \frac{P^-(t)}{\eta_d}) + M.(I_{\max}(t) + I_{\min}(t));\ \forall t. \tag{32}$$

To sum up, the reformulated MINLP model for optimal PV and BES sizing problem comprises the objective function (1) subject to (7), (12)–(14), and (16)–(32). Concretely, the proposed reformulation reduces the number of nonlinear constraints and the bilinear term of (19) is the only nonlinearity of the model.

The fact that current off-the-shelf versions of state-of-the-art solvers (e.g., CPLEX and Gurobi) can solve MILP problems efficiently motivates us to further propose an MILP model for the optimal PV and BES sizing problem.

C. Relaxed MILP Model

A McCormick relaxation technique is applied to develop the MILP model of the optimal PV and BES sizing problem [23]. Accordingly, the bilinear constraint of (19) can be replaced by four McCormick envelops modeled by (33)–(36).

$$\omega(t) \ge C_B.\mathrm{SOC}_{\min};\ \forall t \tag{33}$$

$$\omega(t) \ge C_B^{\max}.\mathrm{SOC}(t) + C_B.\mathrm{SOC}_{\max} - C_B^{\max}.\mathrm{SOC}_{\max};\forall t \tag{34}$$

$$\omega(t) \le C_B^{\max}.\mathrm{SOC}(t) + C_B.\mathrm{SOC}_{\min} - C_B^{\max}.\mathrm{SOC}_{\min};\forall t \tag{35}$$

$$\omega(t) \le C_B.\mathrm{SOC}_{\max};\ \forall t. \tag{36}$$

Inequality constraints (33) and (34) are called McCormick underestimators, while (35) and (36) are called McCormick overestimators.

The advantage of McCormick relaxation over other approximation techniques is that the relaxed MILP model fully contains the feasibility region of the original MINLP model. Ideally, the McCormick envelops represent a convex hull for the MINLP feasibility region [23].

To summarize, Fig. 2 shows the procedure of three proposed models in a single flowchart. After obtaining the optimal sizes for battery and PV systems as continuous values, they are rounded up to the closest available standard discrete sizes.

III. Case Study

A. Building Description and Simulation Setup

Unless stated otherwise, an archetypal residential building situated in Luxembourg is chosen to demonstrate the effectiveness of the proposed models. The annual per unit output of the PV in Luxembourg is obtained from [24]. Fig. 3 plots per unit power production of PV with a resolution of 1 h. Fig. 4 shows the electricty consumption of the building. The hourly data were collected form CREOS (main distribution electricity utility in Luxembourg) database [25]. It can be easily observed that, in colder seasons, the electricity consumption is larger while the PV production is lower than in warmer seasons. The yearly electricity consumption of the building is 4738 kW·h.

The environmental impacts have been calculated using the life cycle assessment methodology, and aggregated into a single score, characterizing the overall impact, as follows. Lifecycle inventory data has been extracted from the Ecoinvent (v3.5) database. In particular, the following inventories were used: "Market for electricity, low voltage, (Luxembourg)," "Photovoltaic slanted-roof installation, multi-Si (Global)," and "Battery

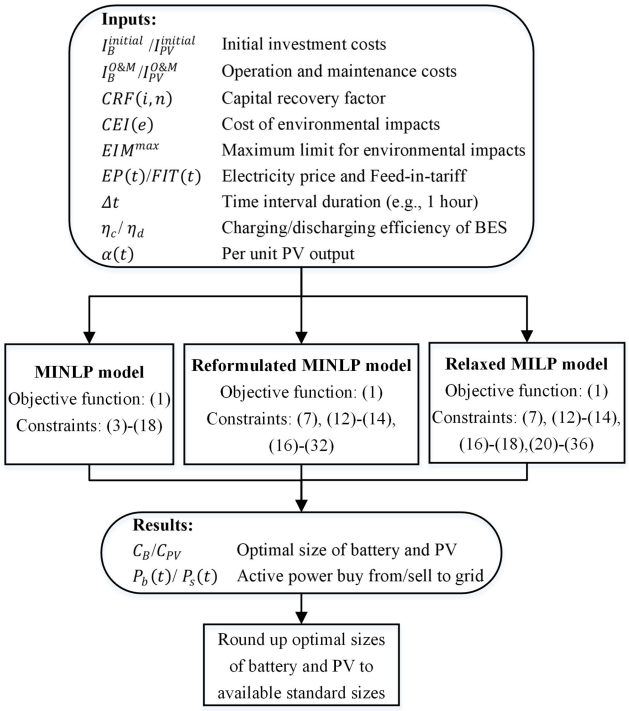

Fig. 2. Flowchart of the proposed models.

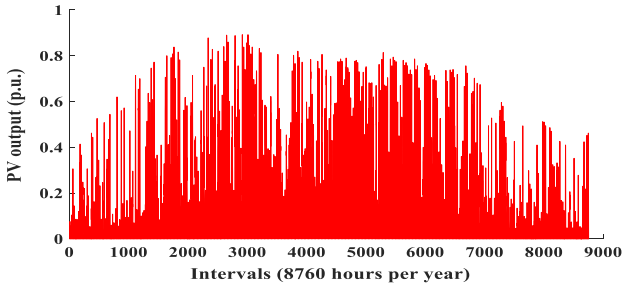

Fig. 3. Yearly per unit power production of PV.

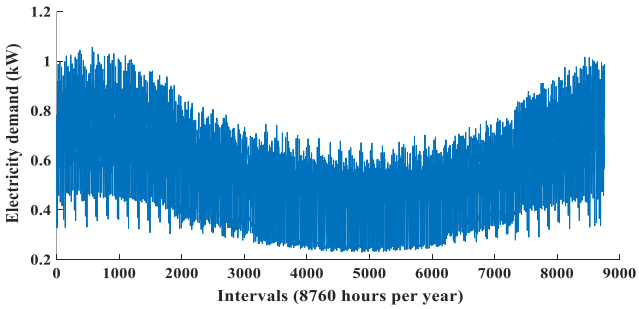

Fig. 4. Yearly electricity consumption of the residential building.

cell, Li-ion (Global)" [26]. The environmental scores are calculated in a sequence of distinct steps. First, the lifecycle inventories, which contain thousands of environmental flows (emissions to air, water, soil, or raw material extraction), are characterized into a series of so-called "midpoint" indicators, which convey the environmental stress generated indirectly and directly by

TABLE II
COST OF ENVIRONMENTAL IMPACTS

	CEI_b (μPt/kWh)	CEI_B (Pt/kWh)	CEI_{PV} (Pt/kWp)
Climate change	15.401	0.00105	0.05434
Ozone depletion	0.098	0.00001	0.00055
Ionizing radiation, HH	2.281	0.00004	0.00233
Photochemical ozone formation, HH	0.866	0.00026	0.00955
Respiratory inorganics	2.853	0.00044	0.01714
Non-cancer human health effects	1.680	0.00171	0.02824
Cancer human health effects	2.973	0.00078	0.02561
Acidification terrestrial and freshwater	3.932	0.00090	0.01737
Eutrophication freshwater	7.476	0.00148	0.02254
Eutrophication marine	0.473	0.00008	0.00266
Eutrophication terrestrial	2.685	0.00015	0.00535
Ecotoxicity freshwater	0.220	0.00019	0.00391
Land use	0.210	0.00002	0.00080
Water scarcity	0.688	0.00012	0.01549
Resource use, energy carriers	12.331	0.00067	0.03218
Resource use, mineral and metals	0.800	0.00367	0.10676
Climate change-fossil	0.000	0.00000	0.00000
Climate change-biogenic	0.000	0.00000	0.00000
Climate change-land use and transform	0.000	0.00000	0.00000
Total	54.965	0.01157	0.34482

each system via various impact mechanisms. For example, the "climate change" impact is accounted in kg CO_2 equivalents (a reference unit to convert the set of greenhouse gas emissions into one single indicator) using their global warming potentials over a 100-year horizon as the characterization factors. The characterization method chosen is the one recommended by the EU's Joint Research Centre in the context of the environmental footprint methodology [27]. A normalization step is necessary to aggregate these various scores into a single indicator. Each midpoint indicator is expressed in "points" (Pt), where one point represents the global impact of that category divided by the world population (yielding the global per-capita average for that category). Once expressed in the same unit, results can be aggregated into a single score, as shown in Table II.

The following assumptions are made to solve the optimization models:

1) PV and BES initial costs are set to $I_{\mathrm{PV}}^{\mathrm{initial}} = 1500$ €/kW·p and $I_B^{\mathrm{initial}} = 50$ €/kW·h, which can be financed at an interest rate of $i = 5\%$ [11]. The annual operation and maintenance costs of PV and BES systems are assumed to be 1% and 2% of their investment costs, respectively [28].
2) The warranty period (or the life cycle) of the PV and BES systems are greater than the payback period of the loan. Therefore, the building owner will not pay any replacement cost over the life span of the systems. This is

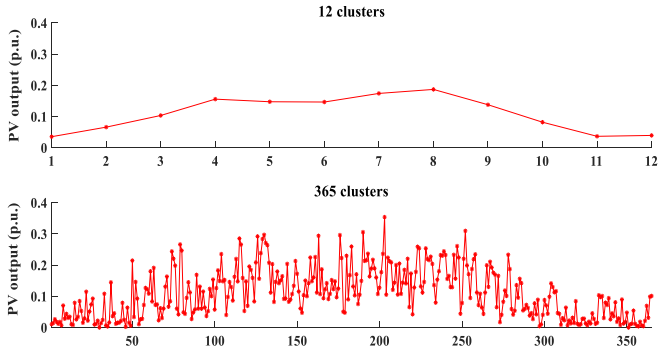

Fig. 5. Clustered data of per unit power production of PV using *K*-means++.

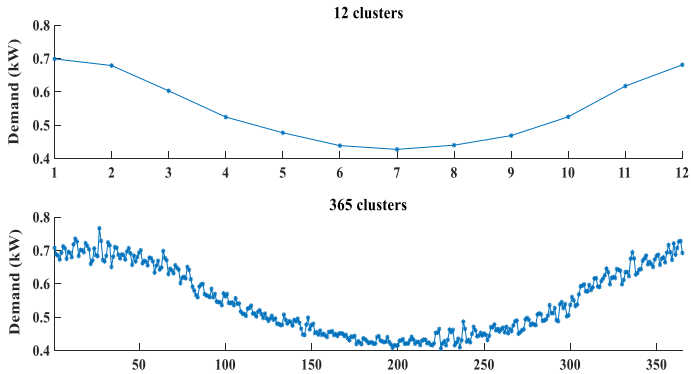

Fig. 6. Clustered data of electricity consumption using *K*-means++.

a sound hypothesis because, for instance, the life cycle of a typical Lithium-Ion battery can be more than 15 years [5], [29].

3) Capacity to power ratio of the battery is small enough to completely charge/discharge the battery between two successive intervals.
4) To reflect the Luxembourg reality, the electricity price, and feed-in-tariff are set to 0.17 €/kW·h and 0.121 €/kW·h, respectively.

To solve MILP and MINLP models, ILOG CPLEX 12.9 and Baron 19 are, respectively, used. All solver options are set to defaults except CPLEX parallel computing options "cpx_param_parallelmode" and "cpx_param_threads," which are, respectively, set to 1 and 48. We used a full node of a high-performance computer (up to 187-GB-RAM) with 48 Intel Skylake @ 2.1GHz cores per node.

B. Numerical Results Without Environmental Impacts

A *K*-means++ algorithm is first used to reduce the size of the PV production and electricity consumption datasets, and to verify the scalability of the proposed models [30]. Initial hourly data of PV production and electricity consumption, which are shown in Figs. 3 and 4, are squeezed into monthly (with 12 clusters) and daily (with 365 clusters) datasets. The occurrence time of the data is taken into account during the clustering process. That is, the time-dependent behavior is preserved in final clusters. The reduced datasets of PV production and electricity consumption are depicted in Figs. 5 and 6, respectively.

We first run a profit-driven optimization, which ignores the environmental impacts limit (18). The so-obtained simulation results for the reformulated MINLP model and the McCormick-based MILP model are provided in Table III. It can be observed that the optimal size of the PV and BES systems depend to a certain extent on the number of intervals. Intuitively, one can expect that the larger the dataset is, the more accurate the decisions will be. It also can be noticed that the solution time of the MILP model is expectedly smaller than that of the MINLP model. As a matter of fact, for the case of 8760 intervals, the MINLP model is unable to find any feasible solution even after 1 00 000 s.

TABLE III
RESULTS FOR DIFFERENT INTERVALS IGNORING ENVIRONMENTAL IMPACTS

Number of intervals		MINLP (reformulated)	MILP (McCormick)
12	Objective Function [€/year]	706.682	706.682
365		795.791	795.791
8760		-	863.364
12	Optimal BES size [kWh]	0.974	0.974
365		0.519	0.519
8760		-	0
12	Optimal PV size [kWp]	4.935	4.935
365		4.935	4.935
8760		-	4.935
12	Cost of buying electricity [€/year]	83.713	83.713
365		256.578	256.578
8760		-	530.097
12	Revenue for selling electricity [€/year]	102.108	102.108
365		183.627	183.627
8760		-	387.021
12	Total CPU time [Seconds]	23.1	1.32
365		7,776	12.3
8760		-	65.2

Furthermore, it is important to remark that the optimal size of the PV does not depend on the number of intervals. This is due to the fact that, in this case study, the net zero energy constraint (17), which is independent from the number of intervals, is binding.

Considering the reformulated MINLP solution as the accurate reference, the McCormick-based MILP model provides similar solutions for the case of 12 and 365 intervals. This proves empirically that the McCormick relaxation is tight enough to provide the global optimal solution for the size of the PV and BES systems.

Fig. 7 shows a 3-D visualization of the McCormick relaxation for the bilinear term of (19). The shape of the latter term is depicted in Fig. 7(a) and allows us to observe that the non-linearity is mild. Fig. 7(b) and 7(c) visualizes the McCormick overestimators and underestimators, respectively. To make the maximum deviation observable, a side view from the angle of an observer situated on the intersection line of the underestimator planes is depicted in Fig. 7(d). As revealed by the case study

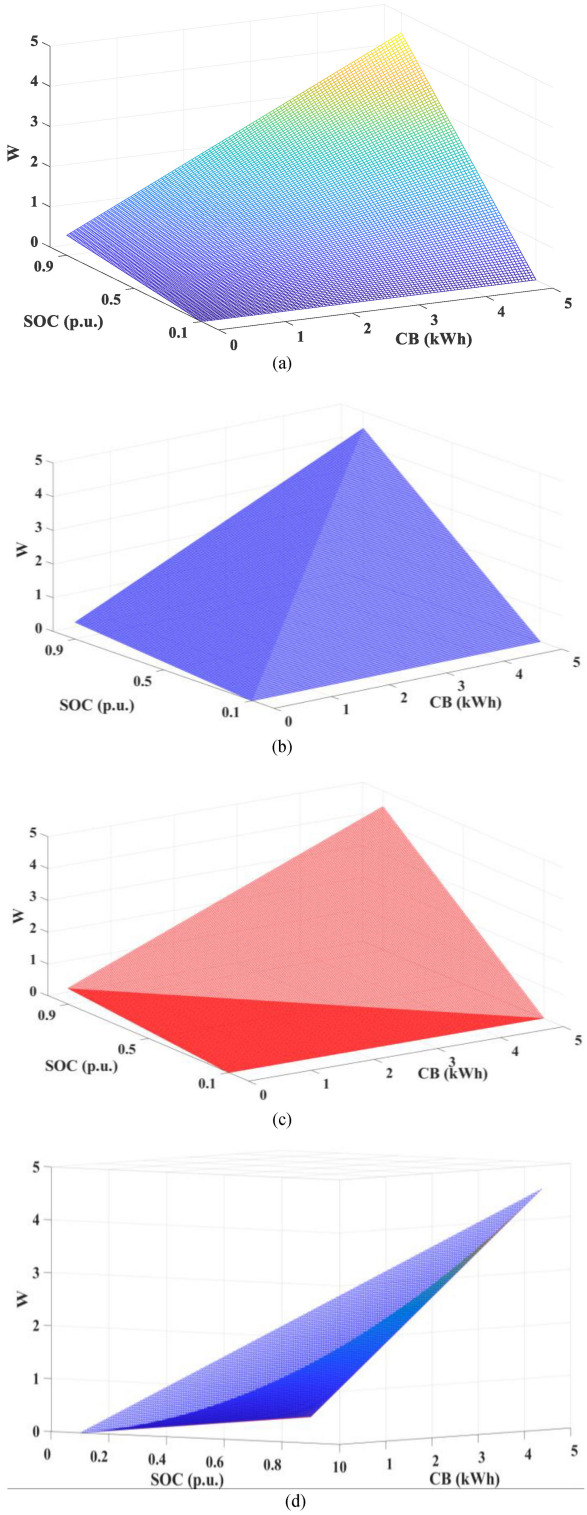

Fig. 7. 3-D visualization of McCormick envelops: (a) bilinear term, (b) overestimators, (c) underestimators, and (d) side view of the envelopes.

and visualized by these 3-D figures, the McCormick relaxation is sufficiently tight to converge in practice to the global optimum of the PV/BES sizing problem.

The SOC of the battery for the case of 365 intervals is shown in Fig. 8. Comparing Fig. 8 with Figs. 3 and 4, one can conclude

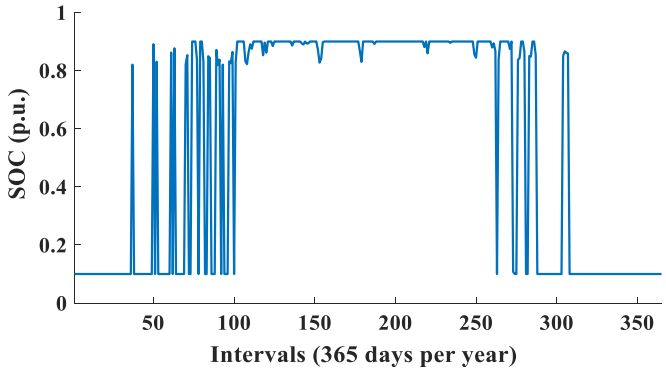

Fig. 8. SOC of the battery for the case of 365 intervals.

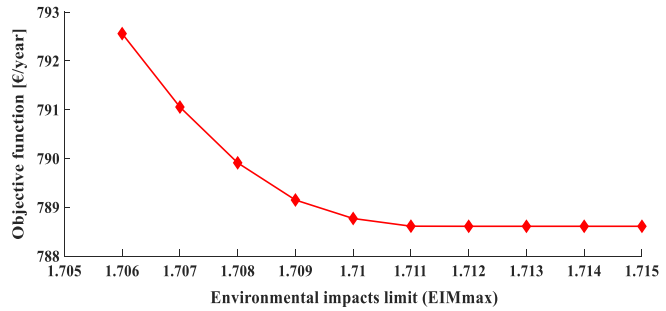

Fig. 9. Sensitivity analysis of the proposed model to the environmental impact constraint for the case of 365 intervals.

that in the warmer seasons, when the electricity consumption is low, the battery stays fully charged more often. However, in the colder seasons when the electricity consumption is high, the battery stays fully discharged as it primarily supplies the demand.

C. Numerical Results Including Environmental Impacts

1) Residential Building: Now the two models are solved including the environmental constraint (18). To analyze the effect of this constraint, a sensitivity analysis is performed as shown in Fig. 9. This figure displays the objective function of the problem with respect to different values of $\mathrm{EIM}^{\max}$ for the case of 365 intervals. Interestingly, if $\mathrm{EIM}^{\max} < 1.706$, the problem becomes infeasible due to incompatibility between the net zero energy constraint (17) and the environmental constraint (18). For the values of $\mathrm{EIM}^{\max}$ larger than 1.711, constraint (18) is inactive and the objective function does not change. For the case of $1.706 \leq \mathrm{EIM}^{\max} \leq 1.711$, constraint (18) is binding and the optimal solution depends on the value of $\mathrm{EIM}^{\max}$ (see Fig. 9). In other words, $\mathrm{EIM}^{\max}$ is an adjustable parameter enabling to tradeoff the environmental impacts and the economical objective. It can be concluded that the desired value of $\mathrm{EIM}^{\max}$ should be selected according to the building owner's willingness-to-pay for environmental impacts.

2) Commercial Building: To further demonstrate the effectiveness of the proposed model, a small commercial building with variable electricity price is considered. The assumed daily

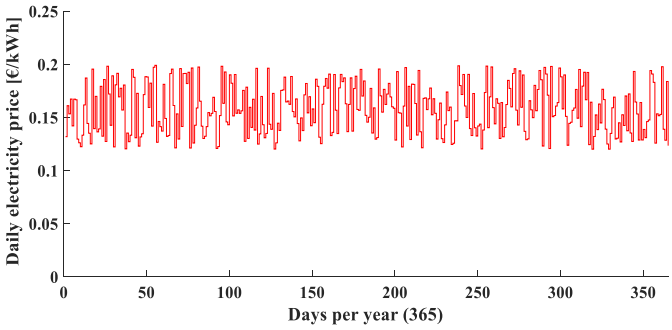

Fig. 10. Daily electricity price of the commercial building.

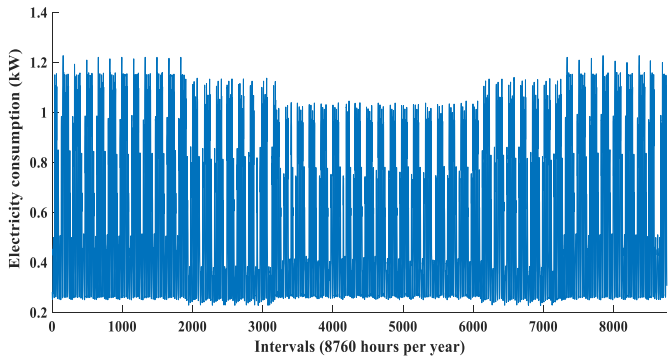

Fig. 11. Hourly electricity consumption of the commercial building.

TABLE IV
RESULTS OF MILP MODEL FOR COMMERCIAL BUILDING WITH HOURLY DATA

	$EIM^{max} = 1.876$	$EIM^{max} = 1.870$
Objective Function [€/year]	828.281	840.792
Optimal BES size [kWh]	1.220	2.580
Optimal PV size [kWp]	4.918	4.924
Cost of buying electricity [€/year]	458.823	412.409
Revenue for selling electricity [€/year]	351.845	315.443
Total CPU time [Seconds]	108.9	112.2

electricity prices are shown in Fig. 10. Fig. 11 shows the hourly electricity consumption data for the commercial building, which is collected form CREOS database [25]. In comparison to the electricity consumption of the residential building (see Fig. 4), a weekly pattern of consumption is obvious in the consumption profile of commercial building (see Fig. 11). Since the commercial building is also located in Luxembourg, the same solar radiation (PV output) and cost of environmental impacts are considered.

The simulation results for the case of hourly data (8760 intervals) are shown in Table IV. For $1.870 \leq \mathrm{EIM}^{\max} \leq 1.876$, constraint (18) is binding and the optimal solution depends on the value of $\mathrm{EIM}^{\max}$. It can be concluded that consideration of

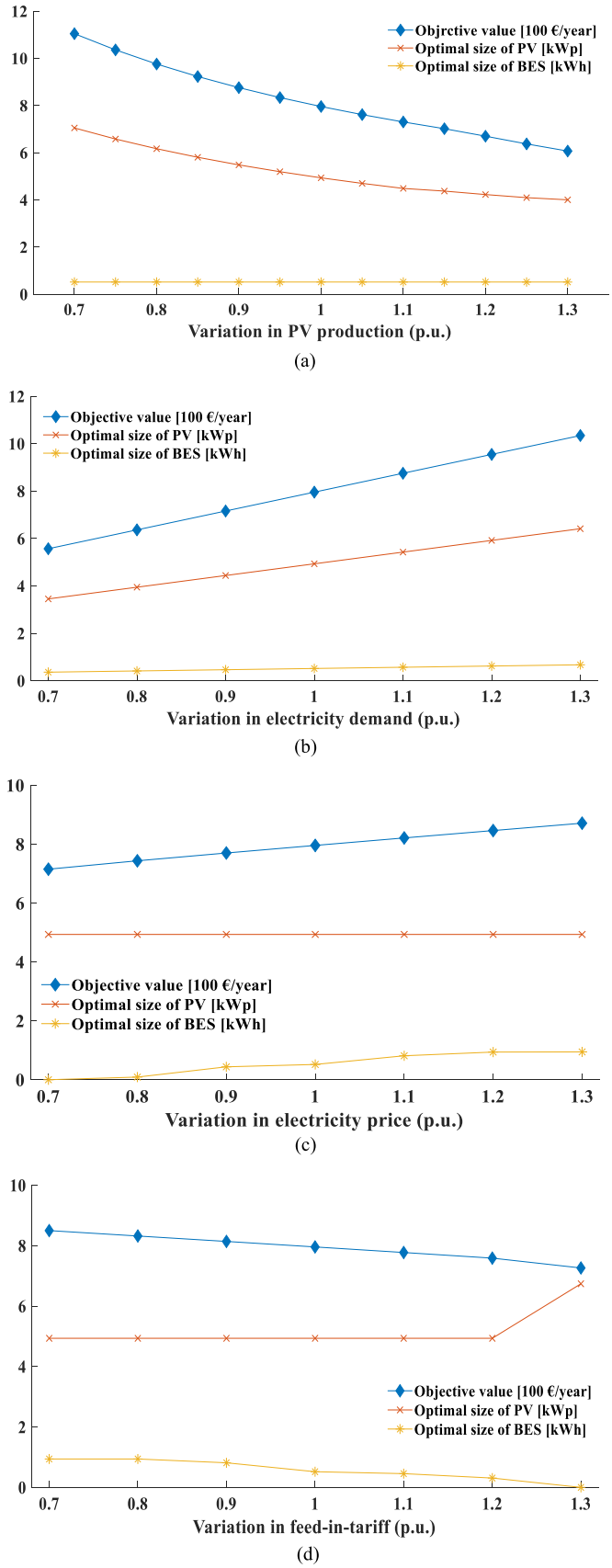

Fig. 12. Sensitivity analysis with respect to ±30% deviation in different inputs for the case of 365 intervals: (a) PV production, (b) electricity demand, (c) electricity price, and (d) feed-in-tariff.

environmental impact constraint ($\mathrm{E\,IM}^{\max} = 1.870$) results in a larger objective value. However, it reduces the amount of electricity bought from the grid by investing in larger PV and BES systems, and consequently, it reduces the overall environmental impacts.

D. Sensitivity Analysis

For the case of the residential building with 365 intervals and $\mathrm{E\,IM}^{\max} = 1.711$, a complete sensitivity analysis is performed. Sensitivity of outputs with respect to $\pm 30\%$ deviation in PV production, electricity consumption, electricity price, and feed-in-tariff, are shown in Fig. 12(a)-(d), respectively. As illustrates in Fig. 12(a), by increasing the PV production from -30% to $+30\%$, the objective value and the optimal size of PV panel are decreased, while the optimal size of the BES system is constant. That is due to the fact that a smaller PV panel is sufficient to fulfill the definition of ZEB (constraint (17)) when the solar radiation (PV output) is higher. As shown in Fig. 12(b), by increasing the electricity demand from -30% to $+30\%$, the objective value and the optimal size of PV panel are considerably increased (to meet ZEB constraint), while the optimal size of the BES system is slightly incremental. It is illustrated in Fig. 12(c) that increasing the electricity price results in a nonlinear increment in the optimal size of the BES system while the PV size is constant. Reducing the electricity price by 30% results in zero investment in the BES system. Finally, by increasing the feed-in-tariff from -30% to $+20\%$, the optimal size of the PV system is fixed while a smaller BES system is desired. Increasing the electricity price by 30% results in investment in a larger PV panel, yet no BES system is desired [see Fig. 12(d)]. These figures show in general smooth variations (and sometimes rather steady values) of optimal PV/BES sizes as parameters change.

IV. Conclusion

This article has proposed an enhanced and rigorous mathematical model of the optimal PV and BES sizing problem in a nearly ZEB. A key original feature of the model is the inclusion of the environmental impacts of buying electricity from the grid and manufacturing PV and BES systems. In addition, an adjustable parameter has been proposed to quantitatively consider the building owner's willingness-to-pay for environmental impacts.

The initial MINLP model has been reformulated in an innovative manner so as to accumulate its nonlinearity in a single constraint per time interval. Afterward, the reformulated model has been linearized to an MILP problem exploiting McCormick relaxation techniques.

The numerical results using archetypal residential and commercial buildings in Luxembourg show that the MINLP model does not scale well to high time interval resolution, even for a problem that pertains to the planning stage. More importantly, extensive simulation results reveal that the proposed McCormick-based MILP problem formulation yields high accuracy results with light computing effort, scaling well to practical, high time resolution modeling. The paper has presented graphical insights underpinning the high accuracy of the MILP problem.

The outcomes of a sensitivity analysis have indicated a rather smooth and little dependence of optimal PV and BES sizes on changes of key parameters. Accordingly, the proposed approach appears as sufficiently mature to inform on PV and BES decisions for the construction of new fully electric-consumption ZEBs. The proposed approach is generic and can be easily adapted to the planning of microgrids operating in grid-connected mode.

The extent of benefits of the proposed approach is obviously location-dependent; however, substantially higher financial and environmental gains are expected in sunnier places than Luxembourg, where solar radiation is slightly below the world average.

Further extensions of this approach regard nonfully electric-consumption buildings, where thermal loads and thermal production/storage elements are present and have to be jointly optimized with PV and BES. In locations with less favorable climatic conditions, achieving the ZEB requirement, may entail cooptimizing the above decisions and energy efficiency measures (e.g., insulation).

References

[1] European Parliament, "Directive 2010/31/EU on the energy performance of buildings (EPBD) – recast," *Off. J. Eur. Union*, vol. 18, no. 6, 2010, Art. no. L153.

[2] S. Rafii-Tabrizi, J.-R. Hadji-Minaglou, F. Scholzen, and F. Capitanescu, "Optimal operation of nearly zero energy buildings using mixed integer linear programming," presented at the International Conference on Smart Energy Systems and Technologies, Istanbul, Turkey, 2019.

[3] F. M. Vieira, P. S. Moura, and A. T. de Almeida, "Energy storage system for self-consumption of photovoltaic energy in residential zero energy buildings," *Renew. Energy*, vol. 103, pp. 308–320, 2017.

[4] M. R. Sarker and M. A. Ortega-Vazquez, "Optimal investment strategy in photovoltaics and energy storage for commercial buildings," in *Proc. IEEE Power Energy Soc. General Meeting*, 2015, pp. 1–5.

[5] O. Ciftci, M. Mehrtash, F. Safdarian, and A. Kargarian, "Chance-constrained microgrid energy management with flexibility constraints provided by battery storage," in *Proc. IEEE Texas Power Energy Conf.*, 2019, pp. 1–6.

[6] O. Ciftci, M. Mehrtash, and A. K. Marvasti, "Data-driven nonparametric chance-constrained optimization for microgrid energy management," *IEEE Trans. Ind. Informat.*, vol. 16, no. 4, pp. 2447–2457, Apr. 2020.

[7] K. Heine, A. Thatte, and P. C. Tabares-Velasco, "A simulation approach to sizing batteries for integration with net-zero energy residential buildings," *Renew. Energy*, vol. 139, pp. 176–185, 2019.

[8] H. Lund, A. Marszal, and P. Heiselberg, "Zero energy buildings and mismatch compensation factors," *Energy Buildings*, vol. 43, no. 7, pp. 1646–1654, 2011.

[9] C. Wu, A. Mohammadi, M. Mehrtash, and A. Kargarian, "Non-parametric joint chance constraints for economic dispatch problem with solar generation," in *Proc. IEEE Texas Power Energy Conf.*, 2019, pp. 1–6.

[10] H. Gong, V. Rallabandi, D. M. Ionel, D. Colliver, S. Duerr, and C. Ababei, "Dynamic modeling and optimal design for net zero energy houses including hybrid electric and thermal energy storage," *IEEE Trans. Industry Appl.*, vol. 56, no. 4, pp. 4102–4113, Jul./Aug. 2020.

[11] V. Sharma, M. H. Haque, and S. M. Aziz, "Energy cost minimization for net zero energy homes through optimal sizing of battery storage system," *Renew. Energy*, vol. 141, pp. 278–286, 2019.

[12] L. Bhamidi and S. Sivasubramani, "Optimal sizing of smart home renewable energy resources and battery under prosumer-based energy management," *IEEE Syst. J.*, to be published, doi: 10.1109/JSYST.2020.2967351.

[13] A. Baniasadi *et al.*, "Optimal sizing design and operation of electrical and thermal energy storage systems in smart buildings," *J. Energy Storage*, vol. 28, 2020, Art. no. 101186.

[14] F. Hafiz, D. Lubkeman, I. Husain, and P. Fajri, "Energy storage management strategy based on dynamic programming and optimal sizing of PV panel-storage capacity for a residential system," in *Proc. IEEE/PES Transmiss. Distrib. Conf. Expo.*, 2018, pp. 1–9.

[15] T. Gibon, A. Arvesen, and E. G. Hertwich, "Life cycle assessment demonstrates environmental co-benefits and trade-offs of low-carbon electricity supply options," *Renew. Sustain. Energy Rev.*, vol. 76, pp. 1283–1290, 2017.

[16] T. Gibon, E. G. Hertwich, A. Arvesen, B. Singh, and F. Verones, "Health benefits, ecological threats of low-carbon electricity," *Environ. Res. Lett.*, vol. 12, no. 3, 2017, Art. no. 034023.

[17] G. Luderer *et al.*, "Environmental co-benefits and adverse side-effects of alternative power sector decarbonization strategies," *Nature Commun.*, vol. 10, no. 1, pp. 1–13, 2019.

[18] M. Mehrtash, F. Capitanescu, and P. K. Heiselberg, "An efficient mixed-integer linear programming model for optimal sizing of battery energy storage in smart sustainable buildings," in *Proc. IEEE Texas Power Energy Conf.*, 2020, pp. 1–6.

[19] Y. Cao, S. B. Lee, V. R. Subramanian, and V. M. Zavala, "Multiscale model predictive control of battery systems for frequency regulation markets using physics-based models," *J. Process Control*, vol. 90, pp. 46–55, 2020.

[20] D. Venkatramanan and V. John, "Dynamic modeling and analysis of buck converter based solar PV charge controller for improved MPPT performance," *IEEE Trans. Industry Appl.*, vol. 55, no. 6, pp. 6234–6246, Nov./Dec. 2019.

[21] B. Zakeri and S. Syri, "Electrical energy storage systems: A comparative life cycle cost analysis," *Renew. Sustain. Energy Rev.*, vol. 42, pp. 569–596, 2015.

[22] S. Rauner and M. Budzinski, "Holistic energy system modeling combining multi-objective optimization and life cycle assessment," *Environ. Res. Lett.*, vol. 12, no. 12, 2017, Art. no. 124005.

[23] A. Tsoukalas and A. Mitsos, "Multivariate McCormick relaxations," *J. Global Optim.*, vol. 59, no. 2–3, pp. 633–662, 2014.

[24] Photovoltaic Geographical Information System. Accessed on: Oct. 12, 2019. [Online]. Available: https://re.jrc.ec.europa.eu/pvg_tools/en/tools.html

[25] Provision of customers based on synthetic profiles. [Online] Available: https://www.creos-net.lu/fournisseurs/electricite/profils-synthetiques.html

[26] G. Wernet, C. Bauer, B. Steubing, J. Reinhard, E. Moreno-Ruiz, and B. Weidema, "The ecoinvent database version 3 (Part I): Overview and methodology," *Int. J. Life Cycle Assessment*, vol. 21, no. 9, pp. 1218–1230, 2016.

[27] European-Commission. "Guidance document, -guidance for the 13development of product environmental footprint category rules," (PEFCRs), version 6.3, Dec. 14, 2017.

[28] K. B. Lindberg, D. Fischer, G. Doorman, M. Korpås, and I. Sartori, "Cost-optimal energy system design in Zero Energy Buildings with resulting grid impact: A case study of a German multi-family house," *Energy Buildings*, vol. 127, pp. 830–845, 2016.

[29] G. Lorenzi, R. da Silva Vieira, C. A. S. Silva, and A. Martin, "Techno-economic analysis of utility-scale energy storage in island settings," *J. Energy Storage*, vol. 21, pp. 691–705, 2019.

[30] D. Arthur and S. Vassilvitskii, "K-Means++: The advantages of careful seeding," in *Proc. 18nth Annu. ACM-SIAM Symp. Discrete Algorithms*, 2007, pp. 1027–1035S.